

Wrinkling Prediction Procedure in Thin Sheet Metal Forming Processes with Adaptive Mesh Refinement

Part I : Contact free wrinkling

Project Title Modelling of Sheet Metal Forming

Project Number ME97033

Cluster Modelling of Sheet Metal Forming

Author A. Selman
 University of Twente
 Netherlands Institute *for* Metals Research

Project Leaders A.H. van den Boogaard

Cluster co-ordinator J. Huetink

Research Assistant T. Meinders

Reference WB.99 / NIMR-0183

December ' 99

Contents

1. Introduction
2. Wrinkling Analysis
3. Wrinkling along a principal axis
4. A simple wrinkling criterion
5. Wrinkling indicator
6. Adaptive strategy
7. General algorithm for wrinkling prediction
8. General comments
9. References

Appendices

This report is meant to be a comprehensive study on wrinkling prediction. An effort is also made to make it self-containing and computer implementation oriented.

This study has lead to the development of a computer program on wrinkling prediction and adaptive refinement.

1. Introduction

Surface distortions in the form of localised buckles and wrinkles are often observed in sheet metals during stamping and other forming operations. In fact, wrinkling is becoming one of the most troublesome modes of failure in sheet forming mainly because of the trend towards thinner, high-strength sheet metals. Therefore, the critical conditions which promote the initiation of wrinkling are of fundamental significance to the design of deep drawn components and may be incorporated in a predictive model for FE simulation.

The methods used in the past to predict wrinkling failures in sheet metals have been mostly empirical (e.g. Yoshida Buckling Test which consists of subjecting a square flat specimen to diagonal tension, as shown in Figure 1. Buckling eventually develops in the central region of the specimen and attempts are made to correlate buckle heights and buckling loads with various material properties). The Yoshida buckling test and other similar empirical methods have, unfortunately, proved to be inadequate for predicting observed trends.

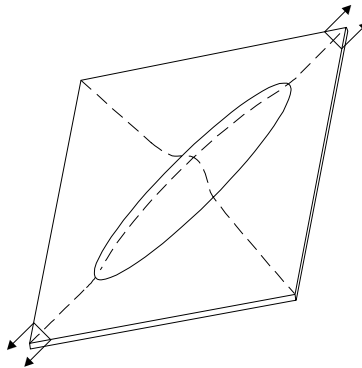


Figure 1. Yoshida buckling test.

A more recent approach for the analysis of local wrinkling has been presented by Hutchinson and Neale (1985). It consists of formulating the problem within the context of plastic bifurcation theory for thin shell elements.

In this work the analysis of Hutchinson and Neale (1985) and its extension by Neale (1989) to account for more general constitutive models (e.g. anisotropy) is used.

2. Wrinkling Analysis

We consider a sheet element (Figure 2) which, in the current stage of forming, has attained a doubly curved state with principal radii of curvature (R_1, R_2) and thickness (t), all assumed to be constant over the region of the sheet being examined for susceptibility to local wrinkling.

The stress state prior to wrinkling is assumed to be uniform membrane state over the local region being examined for wrinkling.

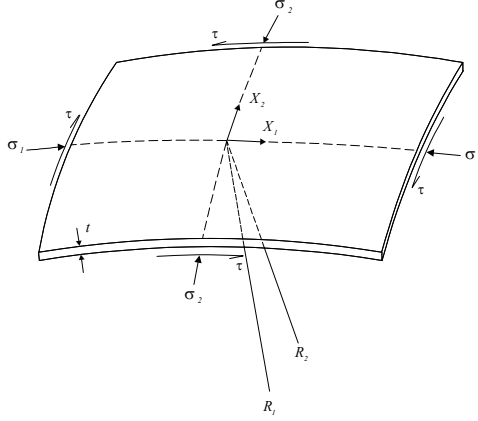


Figure 2. Geometry and loading of curved sheet element.

Although the analysis can account for any stress state, we shall for simplicity assume that the principal axes of this uniform membrane stress state coincide with the principal axes of curvature.

Simplifications arise from the fact that the anticipated short-wavelength modes are shallow and can be analysed using Donnell-Mushtari-Vlasov (DMV) shallow shell theory. This theory restricts the analysis to buckling modes having a characteristic wavelength that is large compared to the sheet thickness, yet small compared to the local radii of curvatures.

The investigation is limited to regions of the sheet which are free of any contact.

The basic theory of plastic buckling and relevant relations for the DMV shallow shell theory have been developed by Hutchinson (1974). The application of this theory to sheet wrinkling was first carried out by Hutchinson and Neale (1985) and is briefly recapitulated here.

According to this analysis, buckling from the uniform membrane state described above gives rise to the following incremental stretching $\dot{E}_{\alpha\beta}$ and bending $\dot{K}_{\alpha\beta}$ strains

$$\dot{E}_{\alpha\beta} = \frac{I}{2} (\dot{U}_{\alpha,\beta} + \dot{U}_{\beta,\alpha}) + b_{\alpha\beta} \dot{W} \quad (1)$$

$$\dot{K}_{\alpha\beta} = -\dot{W}_{,\alpha\beta} \quad (2)$$

Where \dot{U}_{α} ($\alpha, \beta = 1, 2$) are the incremental displacements in the principal surface coordinate directions (x_1, x_2) , \dot{W} is the incremental buckling displacement normal to the middle surface of the sheet, $b_{\alpha\beta}$ ¹ is the curvature tensor of the middle surface in the pre-buckling state and a comma denotes covariant differentiation with respect to a surface co-

¹ The curvature tensor along with the principal curvatures are given in Appendix 3.

ordinate. The above incremental strains lead to incremental stress resultants $\dot{N}_{\alpha\beta}$ and bending moments $\dot{M}_{\alpha\beta}$ at buckling. These are given by

$$\dot{N}_{\alpha\beta} = t \bar{L}^{\alpha\beta\kappa\gamma} \dot{E}_{\alpha\beta} \quad (3)$$

$$\dot{M}_{\alpha\beta} = \frac{t^3}{12} \bar{L}^{\alpha\beta\kappa\gamma} \dot{K}_{\alpha\beta} \quad (4)$$

where $\bar{L}^{\alpha\beta\kappa\gamma}$ are the plane-stress incremental moduli relating stress increments $\dot{\sigma}_{\alpha\beta}$ to strain increments $\dot{\epsilon}_{\alpha\beta}$ through $\dot{\sigma}_{\alpha\beta} = \bar{L}^{\alpha\beta\kappa\gamma} \dot{\epsilon}_{\kappa\gamma}$. These moduli, which depend on the particular constitutive theory adopted, are uniform throughout the sheet because of the assumption of a homogenous membrane state prior to buckling.

To determine the critical stress state for buckling we use Hutchinson's (1974) bifurcation functional

$$F(\dot{U}, \dot{W}) = \int_S \left[\frac{t^3}{12} \bar{L}^{\alpha\beta\kappa\gamma} \dot{K}_{\alpha\beta} \dot{K}_{\kappa\gamma} + t \bar{L}^{\alpha\beta\kappa\gamma} \dot{E}_{\alpha\beta} \dot{E}_{\kappa\gamma} + N^{\alpha\beta} \dot{W}_{,\alpha} \dot{W}_{,\beta} \right] dS \quad (5)$$

where S is the local area of the sheet over which the wrinkles develop.

The condition $F > 0$ for all admissible fields $\dot{U}_{,\alpha}, \dot{W}$ ensures that bifurcation will not occur. Conversely, bifurcation first becomes possible when $F = 0$ for some non-zero field.

Wrinkling or bifurcation in short wavelength shallow modes is described by the following fields

$$\begin{aligned} \dot{W} &= A t \cos(2\pi \lambda_1 x_1 / l) \cos(2\pi \lambda_2 x_2 / l) \\ \dot{U}_1 &= B t \cos(2\pi \lambda_1 x_1 / l) \sin(2\pi \lambda_2 x_2 / l) \\ \dot{U}_2 &= C t \cos(2\pi \lambda_1 x_1 / l) \sin(2\pi \lambda_2 x_2 / l) \end{aligned} \quad (6)$$

where $l = \sqrt{Rt}$ in which R is identified with either R_1 or R_2 as appropriate, A, B, C are constants representing the relative displacement amplitudes of the mode shape and λ_1, λ_2 are non-dimensional wave numbers. In employing these fields we anticipate that wrinkling occurs over a certain region S of the sheet which spans many wavelengths of the buckling mode. The boundary conditions along the edge of S then become unimportant. In this sense, the analysis is a local one.

The analysis involves substituting the above fields (6) into the bifurcation functional (5) and integrating over S . In so doing we use the incremental stretching $\dot{E}_{\alpha\beta}$ and bending

$\dot{K}_{\alpha\beta}$ strains relations with $b_{11} = 1/R_1$, $b_{22} = 1/R_2$ as well as $N^{11} = -t\sigma_1$, $N^{22} = -t\sigma_2$. We also make use of the following formulas

$$\left. \begin{aligned} & \int_S [\sin(2\pi \lambda_1 x_1 / l) \sin(2\pi \lambda_2 x_2 / l)]^2 dS \\ & \int_S [\cos(2\pi \lambda_1 x_1 / l) \cos(2\pi \lambda_2 x_2 / l)]^2 dS \end{aligned} \right\} = \beta S \quad (7)$$

where $\beta = 1/4$ if both λ_1 and λ_2 are nonzero, and $\beta = 1/2$ if either λ_1 or λ_2 is zero.

The bifurcation functional can then be written as

$$F = \beta S t \left(\frac{t}{l}\right)^2 \mathbf{u}^T \mathbf{M} \mathbf{u} \quad (8)$$

where $\mathbf{u} = \{A, B, C\}$ is the buckling displacement amplitude vector and the matrix \mathbf{M}^2 depends on the local geometry and incremental moduli.

Buckling is possible when the associated functional $F = 0$. In view of (8) this first occurs when the determinant of \mathbf{M} vanishes.

To determine the critical stress values σ_1^{cr} , σ_2^{cr} for which short wavelength buckling first occurs, we minimise this determinant with respect to the waveform parameters λ_1 and λ_2 and set the minimum to zero. The values of λ_1^{cr} and λ_2^{cr} so obtained describe the corresponding critical buckling pattern.

The three equations to be solved are

$$\left\{ \begin{aligned} \det \mathbf{M} &= 0 \\ \frac{\partial \det \mathbf{M}}{\partial \lambda_1} &= 0 \\ \frac{\partial \det \mathbf{M}}{\partial \lambda_2} &= 0 \end{aligned} \right. \quad (9)$$

² The components of the matrix \mathbf{M} are given in Appendix 4 along with the notation used for the incremental moduli.

In view of the complexity of the equations involved, closed form analytic solutions cannot generally be obtained. Hence, numerical solutions are generated by solving (9) using Newton-Raphson technique. However, a severe sensitivity to the initial guess is encountered. This sensitivity stems from the fact that many modes of buckling correspond to nearly the same level of stress.

3. Wrinkling along a principal axis

For the pre-wrinkling geometry and stress state considered in the previous section, wrinkling will in most cases be aligned with one of the principal curvatures (stress) directions. In such a case either λ_1 or λ_2 is zero and the previous analysis simplifies considerably. For example, for **wrinkling perpendicular to the 1-direction** i.e. $\lambda_2 = 0$, $b_{12} = 0$, $b_{11} \neq 0$, $b_{22} \neq 0$, $\dot{U}_1 = 0$, $\dot{U}_2 = 0$ and $\dot{W} = A \cos(2\pi \lambda_1 x_1 / l)$, hence the system of equations to be solved reduces to

$$\begin{cases} \det \mathbf{M} = 0 \\ \frac{\partial \det \mathbf{M}}{\partial \lambda_1} = 0 \end{cases} \quad (10)$$

with the coefficients of matrix \mathbf{M} reducing to

$$\begin{aligned} M_{11} &= \frac{l}{12} \left(\frac{t}{l} \right)^2 L_{11} \lambda_1^4 + L_{11} \left(\frac{l}{R_1} \right)^2 + L_{22} \left(\frac{l}{R_2} \right)^2 + 2 L_{12} \left(\frac{l}{R_1} \right) \left(\frac{l}{R_2} \right) - \sigma_1 \lambda_1^2 \\ M_{22} &= L_{11} \lambda_1^2 \\ M_{33} &= L_{12} \lambda_1^2 \\ M_{12} &= M_{21} = L_{11} \lambda_1 \frac{l}{R_1} + L_{12} \lambda_1 \frac{l}{R_2} \\ M_{13} &= M_{31} = M_{23} = M_{32} = 0 \end{aligned} \quad (11)$$

Using (11) the system of equations (10) becomes

$$\begin{cases} \frac{l}{12} \left(\frac{t}{l} \right)^2 L_{11}^2 \lambda_1^4 - \sigma_1 L_{11} \lambda_1^2 + (L_{11} L_{22} - L_{12}^2) \left(\frac{l}{R_2} \right)^2 = 0 \\ \frac{2}{3} \left(\frac{t}{l} \right)^2 L_{11}^2 \lambda_1^4 - 6 \sigma_1 L_{11} \lambda_1^2 + 4(L_{11} L_{22} - L_{12}^2) \left(\frac{l}{R_2} \right)^2 = 0 \end{cases} \quad (12)$$

Solving the above set of equations gives the following expression for the critical wrinkling stress

$$\sigma_1^{cr} = \frac{1}{\sqrt{3}} \frac{t}{R_2} (L_{11} L_{22} - L_{12}^2)^{1/2} \quad (13)$$

and the corresponding critical wavelength parameter

$$\lambda_1^{cr} = \left[2\sqrt{3} (L_{11} L_{22} - L_{12}^2)^{1/2} / L_{11} \right]^{1/2} \quad (14)$$

Although σ_2 does not enter explicitly in the critical conditions (13) and (14), it nevertheless does influence wrinkling since the incremental moduli $L_{\alpha\beta}$ depend on σ_2 .

The results (13) suggests that the ratio t/R_2 is the only relevant geometric parameter for wrinkling aligned with the 2-direction. The radius of curvature R_1 perpendicular to the wrinkles does not affect σ_1^{cr} . Similar observations obviously hold for σ_2^{cr} associated with wrinkles lying perpendicular to the 2-direction.

4. A simple wrinkling criterion

A simple wrinkling criterion can be obtained from the foregoing analysis, if we assume that the pre-wrinkling loading history is proportional (or nearly so) and that deformation theory of plasticity can be used to characterise the material behaviour (see Hutchinson's (1974) discussion for arguments supporting the use of deformation theory in plastic bifurcation calculations). If incompressibility is also assumed, the incremental moduli $L_{\alpha\beta}$ according to Hill's (1950) anisotropic yield criterion become

$$\begin{aligned} L_{11} &= \frac{(1+r)^2}{(1+2r)} E_s - (E_s - E_t) \frac{\sigma_1^2}{\sigma_e^2} \\ L_{12} &= \frac{r(1+r)}{(1+2r)} E_s - (E_s - E_t) \frac{\sigma_1 \sigma_2}{\sigma_e^2} \\ L_{22} &= \frac{(1+r)^2}{(1+2r)} E_s - (E_s - E_t) \frac{\sigma_2^2}{\sigma_e^2} \end{aligned} \quad (15)$$

where E_t is the tangent modulus (the slope of the uniaxial stress-strain curve at $\sigma = \sigma_e$) and $E_s = \sigma_e / \varepsilon_e$ is the secant modulus, also obtained from the uniaxial stress-strain curve at the stress level σ_e . The parameter r , widely used in the characterisation of sheet metal anisotropy, is the ratio of the width-to-thickness plastic strain increment in uniaxial in-plane tension.

The effective stress is given by

$$\sigma_e = \left[\sigma_1^2 - \frac{2r}{(1+r)} \sigma_1 \sigma_2 + \sigma_2^2 \right]^{1/2} \quad (16)$$

For the Proportional Loading case $\frac{\sigma_2}{\sigma_1} = \alpha$, the effective stress σ_e can be rewritten as

$$\sigma_e = \left[1 - \frac{2r\alpha}{(1+r)} + \alpha^2 \right]^{1/2} \sigma_1 = \alpha_1 \sigma_1 \quad \text{or} \quad \sigma_e = \alpha_1 \sigma_1 \quad (17)$$

with

$$\alpha_1 = \left[1 - \frac{2r\alpha}{(1+r)} + \alpha^2 \right]^{1/2} \quad (18)$$

For the Proportional Straining case $\frac{\varepsilon_2}{\varepsilon_1} = \rho$, the proportionality coefficient can be rewritten as

$$\alpha = \frac{\sigma_2}{\sigma_1} = \frac{L_{12} + L_{22}\rho}{L_{11} + L_{12}\rho} \quad (19)$$

and using (15) we get

$$\alpha = \frac{1 + \rho + \rho r}{1 + r + \rho r} \quad (20)$$

Finally, we can express σ_e , in terms of ρ , as

$$\sigma_e = \frac{\sqrt{1+2r}}{1+r+\rho r} \left[1 + \frac{2\rho r}{1+r} + \rho^2 \right]^{1/2} \sigma_1 = \bar{\alpha}_1 \sigma_1 \quad (21)$$

with

$$\bar{\alpha}_1 = \frac{\sqrt{1+2r}}{1+r+\rho r} \left[1 + \frac{2\rho r}{1+r} + \rho^2 \right]^{1/2} \quad (22)$$

and the effective strain as

$$\varepsilon_e = \frac{1+r}{\sqrt{1+2r}} \left[1 + \frac{2\rho r}{1+r} + \rho^2 \right]^{1/2} \varepsilon_1 = \bar{\rho}_1 \varepsilon_1 \quad (23)$$

with

$$\bar{\rho}_1 = \frac{1+r}{\sqrt{1+2r}} \left[1 + \frac{2\rho r}{1+r} + \rho^2 \right]^{1/2} \quad (24)$$

Substituting (17) or (21) into (15) and the resulting expression in (13) and (14) gives the critical wrinkling stress as

$$\sigma_1^{cr} = \frac{1+r}{\sqrt{3(1+2r)}} \frac{t}{R_2} \sqrt{E_s E_t} \quad (25)$$

and the critical wavelength parameter as

$$\lambda_1^{cr,2} = \frac{2\sqrt{3}(1+r)\sqrt{E_s E_t}}{\sqrt{(1+2r)} \left[\frac{(1+r)^2}{1+2r} E_s - (E_s - E_t) \frac{1}{\alpha_1^2} \right]} \quad (26)$$

α_1 is to be replaced by $\bar{\alpha}_1$ when proportional straining is used.

We now consider two types of hardening relations. These relations are used to get explicit expressions for the tangent and secant moduli E_t and E_s , which in turn are used to express the critical values in a simplified format.

4.1 Hollomon's law

Hollomon's power law hardening relation is of the following form

$$\sigma_e = K \varepsilon_e^n \quad (27)$$

In the plastic range, we have

$$\left. \begin{aligned} E_t &= \frac{d\sigma_e}{d\varepsilon_e} = n K \varepsilon_e^{n-1} \\ E_s &= \frac{\sigma_e}{\varepsilon_e} = K \varepsilon_e^{n-1} \end{aligned} \right\} \quad (28)$$

or, equivalently, by use of (17) and (27), we can rewrite E_t and E_s as

$$\left. \begin{aligned} E_t &= n K^{1/n} (\alpha_1 \sigma_1)^{1-1/n} \\ E_s &= K \left(\frac{\sigma_e}{K} \right)^{1-1/n} = K^{1/n} (\alpha_1 \sigma_1)^{1-1/n} \end{aligned} \right\} \quad (29)$$

Replacing E_t and E_s by their expressions in (29) gives the critical wrinkling stress (25) as

$$\sigma_1^{cr} = K \left[\frac{1+r}{\sqrt{3(1+2r)}} \frac{t}{R_2} \sqrt{n} \alpha_1^{1-1/n} \right]^n \quad (30)$$

and using Hollomon's law

$$\sigma_e = K \varepsilon_e^n \Rightarrow \bar{\alpha}_1 \sigma_1^{cr} = K (\bar{\rho}_1 \varepsilon_1^{cr})^n \quad (32)$$

gives the critical strain as

$$\varepsilon_1^{cr} = \frac{\sqrt{(1+2r)n}}{\sqrt{3}(1+r+\rho r)} \left(\frac{t}{R_2} \right) \quad (33)$$

In the same way, we can express the critical wave number as

$$\lambda_1^{cr2} = \frac{2\sqrt{3}\sqrt{n}}{\frac{1+r}{\sqrt{1+2r}} - \frac{(1-n)\sqrt{1+2r}}{(1+r)} \frac{1}{\alpha_1^2}} \quad (31)$$

for wrinkling perpendicular to the 1-direction.

Again, in (31) α_1 is to be replaced by $\bar{\alpha}_1$ when proportional straining is used.

4.2 Swift's law

Following the same procedure we now present the expressions for the critical stress, strain and wave numbers when Swift's law is used. This law is expressed by

$$\sigma_e = K(\varepsilon_p + \varepsilon_o)^n \quad (34)$$

During the drawing process, the elastic deformation is negligible compared with the plastic deformation, consequently we can approximate the equivalent plastic deformation at a given point by its plastic deformation, that is

$$\varepsilon_e \approx \varepsilon_p \quad (35)$$

This approximation allows us to express the tangential and secant modulus for this law as

$$\left. \begin{aligned} E_t &= K n (\varepsilon_p + \varepsilon_o)^{n-1} \\ E_s &= \frac{K(\varepsilon_p + \varepsilon_o)^n}{\varepsilon_p} \end{aligned} \right\} \quad (36)$$

Inserting (36) in the general critical stress expression (25) and noting that for Swift's law, the equivalent plastic deformation can be written as a function of the critical wrinkling stress as follows

$$\varepsilon_p = \left(\frac{\alpha_1 \sigma_1^{cr}}{K} \right)^{1/n} - \varepsilon_o \quad (37)$$

It can be shown that the wrinkling critical stress to the power $1/n$ is the positive solution of the following quadratic equation

$$\left(\sigma_1^{cr} \right)^{2/n} \left(\frac{\alpha_1}{K} \right)^{1/n} - \varepsilon_o \sigma_1^{cr} - \frac{(1+r)^2}{3(1+2r)} \left(\frac{t}{R_2} \right)^2 K^2 n \left(\frac{\alpha_1}{K} \right)^{2-1/n} = 0 \quad (38)$$

That positive solution is given by

$$\sigma_1^{cr} = \frac{K}{2^n \alpha_1} \left[\varepsilon_o + \left[\varepsilon_o^2 + 4 n \alpha_1^2 \frac{(1+r)^2}{3(1+2r)} \left(\frac{t}{R_2} \right)^2 \right]^{1/2} \right]^n \quad (39)$$

Using expressions (23) and (37) and the critical stress expression (39) it is possible to determine the corresponding critical deformation by use of Swift's law. Noting that $\alpha_1 = \bar{\alpha}_1^3$, this leads to

$$\varepsilon_1^{cr} = \frac{1}{2 \bar{\rho}_1} \left[\left[\varepsilon_o^2 + 4 n \bar{\alpha}_1^2 \frac{(1+r)^2}{3(1+2r)} \left(\frac{t}{R_2} \right)^2 \right]^{1/2} - \varepsilon_o \right] \quad (40)$$

For consistency reasons α_1 is used in the critical stress determination and $\bar{\alpha}_1$ is used for the critical strain evaluation.

Finally the critical stress is used to evaluate the secant and tangent moduli during bifurcation, to determine the critical wave numbers by use of the general formula (26), which is for convenience rewritten here

³ The same value can be expressed either in terms of α or ρ .

$$\lambda_1^{cr2} = \frac{2\sqrt{3}(1+r)\sqrt{E_s E_t}}{\sqrt{(1+2r)} \left[\frac{(1+r)^2}{1+2r} E_s - (E_s - E_t) \frac{l}{\alpha_1^2} \right]} \quad (41)$$

α_1 is to be replaced by $\bar{\alpha}_1$ when proportional straining is used.

Before proceeding further, we note that in the above expressions of the critical stress, strain and wave parameter σ_1 is set to σ_1^{cr} in the evaluation of the tangent and secant moduli. In so doing it is assumed that at the stress level at wrinkling is the buckling stress, and therefore a conservative evaluation of the critical stress is made. Nonetheless, in Appendix 2, for Hollomon's law's, the critical stress, strain and wave number in both directions, when the pre-wrinkling stress is used in the evaluation of the tangent and secant moduli are given.

5. Wrinkling indicator

Using the wrinkling critical stress and strain values, we define a wrinkling risk factor (perpendicular to the 1-direction) in terms of stress, as

$$f_\sigma = \frac{\sigma_1}{\sigma_1^{cr}} \quad (42)$$

and in terms of strain, as

$$f_\varepsilon = \frac{\varepsilon_1}{\varepsilon_1^{cr}} \quad (43)$$

Therefore a wrinkling risk exists whenever f_σ or f_ε is larger than 1. The risk is more important with larger values of the risk factors.

6. Adaptive strategy

In the adaptive procedure we need to detect the zones (elements) to be refined and determine a new size for those zones (elements). The zones detection is obtained by the use of the wrinkling risk factors (42) or (43). The new mesh size is obtained by the use of the wavelength of the wrinkles

$$L_1 = \frac{l}{\lambda_1} = \frac{\sqrt{R_2 t}}{\lambda_1} \quad (44)$$

to get a new weighted wrinkling mesh size as

$$L^w = \frac{L_1}{m} f_\sigma^{-1} \quad (45)$$

or, when the strain is used

$$L^w = \frac{L_1}{m} f_\varepsilon^{-1} \quad (46)$$

with m being the number of elements we wish to discretise the wave with.

All of the above formulae have developed for wrinkling perpendicular to the 1-direction. For wrinkling perpendicular to the 2-direction, please refer to Appendix 1.

7. General Algorithm for wrinkling prediction

Input the FE model (coordinates and connectivity) and principal stresses (strains)

For each element evaluate if necessary ⁴ the principal curvatures

Depending on the signs of the principal stresses (strains), go to one of the four situations depicted in Figure 3. If Case I is encountered, go to next element. Else

Evaluate the proportionality factors as appropriate

Evaluate the critical stress (strain) and wavelength number ⁵ for wrinkling perpendicular to the 1-direction (Case II)

Evaluate the critical stress (strain) and wavelength number for wrinkling perpendicular to the 2-direction (Case III)

Evaluate the critical stresses (strains) in both directions for Case IV and determine the predominant direction for wrinkling. Once the wrinkling direction is found evaluate the corresponding wavelength number.

Evaluate the risk factor

Evaluate the wrinkling mesh size and go to next element.

⁴ i.e. elements with a non-zero geometric error if the wrinkling prediction algorithm is used in conjunction with the error estimation routine. Otherwise, all curvatures need to be determined.

⁵ depending on the hardening law.

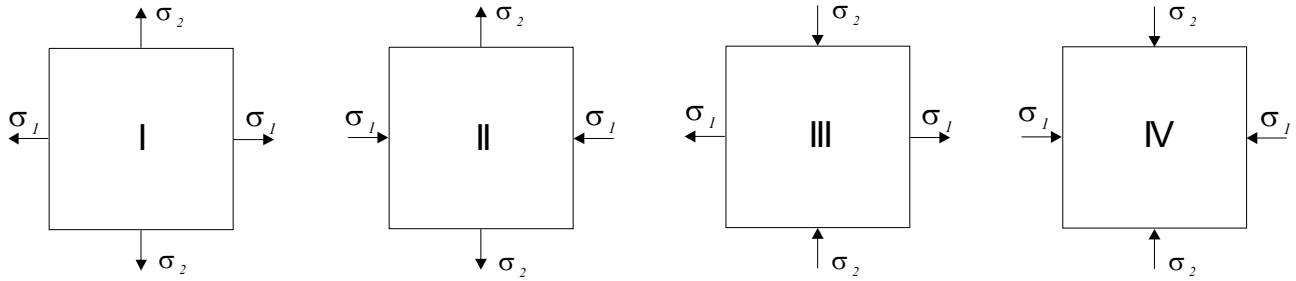


Figure 3. Possible wrinkling directions.

8. General comments

- Many idealisations have been made in developing the simple criterion and their applicability is rather restrictive. Nevertheless, these results do serve as an indication of the influence of local geometry t/R_1 (t/R_2), material properties n, r and loading condition α, ρ on wrinkling. The criterion (33), for example, shows that a decrease in strain hardening or thickness-to-radius ratio decreases the critical strain at wrinkling. On the other hand, the critical strain increases as the strain ratio ρ is reduced. It is therefore not surprising that wrinkling has become a more prominent problem, since the higher strength sheet metals being favoured in recent years tend to be thinner with lower strain hardening.
- It should be noted that the use of the pre-wrinkling stress in the evaluation of E_s and E_t which in turn are used to evaluate the critical stress, strain and wave number has the effect of overestimating the critical values and, consequently, underestimating the wrinkling risk factors.
- Wrinkling is a buckling phenomenon, therefore, it takes place if and only if one of the principal stresses is compressive. Consequently, to keep the computational cost low, a pre-selection of candidate elements for wrinkling is performed before the wrinkling analysis is started. Figure 3 depicts the four possible cases that can be encountered. Obviously in Case I no wrinkling is possible. In Case II wrinkling perpendicular to the 1-direction is possible and consequently σ_1^{cr} , ε_1^{cr} and λ_1^{cr} are to be determined. In Case III wrinkling perpendicular to the 2-direction is possible, therefore σ_2^{cr} , ε_2^{cr} and λ_2^{cr} are to be evaluated. Finally, Case IV is the most demanding as wrinkling is possible in both directions. To determine the dominant wrinkling direction, both possibilities are to be investigated.
- When Hollomon's law is used it can be shown that, depending of the value on the ratio α , one of the two principal stresses dominates the other and initiates wrinkles perpendicular to its direction. The value of the proportionality factor α_o for which the

principal stress σ_2 is predominant over σ_1 is determined by use of (30) and is simply

$$\alpha_0 = \left(\frac{R_1}{R_2} \right)^{1/1-n}.$$

An explicit expression for (α_0) cannot be determined when Swift's law is used. Nonetheless, the evaluation of both σ_1^{cr} and σ_2^{cr} will determine the wrinkling direction.

- As already mentioned, the analysis presented herein is only concerned with doubly curved shells. Therefore, if the wrinkling prediction analysis is used in conjunction with our error estimation routine, an advantage is taken from the fact that zero geometric error element (which means that the element is on a flat surface) is not considered for wrinkling prediction analysis.
- When, for instance, Hollomon's law is used, it can be shown that $f_\epsilon = (f_\sigma)^{1/n}$. Clearly the wrinkling risk factor is different when evaluated using the stress or strain values : when the stress risk factor is smaller than 1, f_ϵ is less than 1 and less than f_σ ($f_\epsilon < f_\sigma < 1$), and conversely if f_σ is larger than 1, f_ϵ is larger than 1 and f_σ ($f_\epsilon > f_\sigma > 1$) (given that n is smaller than 1 for an elasto-plastic law). Therefore, when the deformations are used in the evaluation of the wrinkling risk factors, this has the effect of either damping or amplifying the wrinkling phenomenon. This tendency is caused by the strong relation between the equivalent stress and strain in Hollomon's law.
- It is generally found that the deformation theory, which predicts lower buckling stresses than the corresponding flow theory, gives results which are in better agreement with experiment. For this reason our emphasis has been on the deformation theory predictions. Deformation theory produces more conservative predictions for the onset of wrinkling and is thus more attractive for design purposes. It is now generally favoured over flow theory for the plastic bifurcation analysis of plate and shell structures (Hutchinson 1974).
- When the wrinkling prediction routine is used in conjunction with the error estimation code, the wrinkling size defined in (45) or (46) is to be incorporated with the new thickness and geometric sizes as defined in our report on error estimation to give a global new size for mesh refinement as

$$L^{new} = \max \left[L_{min}, \min(L^w, L^h, L^g) \right]$$

- Given that the present wrinkling analysis is a local one and that it is a post-processing technique, the computational cost is very low.

9. References

R. Hill

A general theory of uniqueness and stability in elastic-plastic solids

J. Mech. Phys. Solids, 6, 236-249, (1958)

J.W. Hutchinson

Plastic buckling

Adv. Appl. Mech., 14, 67-144 (1974).

H. Hayashi, K. Miyauchi and K. Yoshida

Yoshida buckling test : Data sheets

IDDRG, Detroit, (1982)

J.W. Hutchinson and K.W. Neale

Wrinkling of curved thin sheet metal

Plastic Instability, J. Salencon (Ed.), Press Ponts et Chaussees, 71-78, (1985).

H. Ameziane-Hassani

Contribution a la prevision de l'ondulation dans les coques minces elastoplastiques a double courbure

PhD thesis, Universite de Sherbrooke, (1988).

K.W. Neale

Numerical analysis of sheet metal wrinkling

Numiform '89, Thompson et al (Eds.), 501-505, Balkema, Rotterdam, (1989)

K.W. Neale and P. Tugcu

A numerical analysis of wrinkling formation tendencies in sheet metals

Int. J. Num. Meth. Eng., 30, 1595-1608, (1990).

H. Ameziane-Hassani and K. Neale

On the analysis of sheet metal wrinkling

Int. J. Mech. Sci., 33, 13-30, (1991).

S. Brunet, J.L. Batoz and S. Bouabdallah

Sur l'evaluation des risques de plissement locale de pieces industrielles obtenues par emboutissage

Actes du 3eme Colloque National en Calcul des Structures , 753-758, Giens, France (1997).

J.C. Gelin, P. Paquier and N. Boudeau

Prediction of necking and wrinkling in sheet metal forming from the analysis of local equilibrium conditions

Numiform '98, J. Huetink and F.P.T. Baaijens (Eds.), Balkema, Rotterdam, (1998).

A. Selman

Notes on error estimation and adaptive mesh refinement in thin sheet metal forming processes

Internal Report, University of Twente, Faculty of Mechanical Engineering,
WB.99 / NIMR-0154 (1999).

P.M. Naghdi

The theory of shells and plates

Mechanics of Solids II, Vol. 2, S. Flugge and C. Truesdell (Eds.), Springer, (1972).

Appendix 1

Wrinkling perpendicular to the 2-direction

First a recap of the formulae used so far in wrinkling prediction perpendicular to the 1-direction is presented (this also stands as an algorithm for the evaluation of the critical stress, strain and wave number)

Stress	Strain
$\alpha = \sigma_2 / \sigma_1$	$\rho = \varepsilon_2 / \varepsilon_1$
$\alpha_1 = \left[1 - \frac{2r\alpha}{(1+r)} + \alpha^2 \right]^{1/2}$	$\bar{\alpha}_1 = \frac{\sqrt{1+2r}}{1+r+\rho r} \left[1 + \frac{2r\rho}{1+r} + \rho^2 \right]^{1/2}$
<p>Hollomon's Law</p>	<p>Hollomon's Law</p>
$\sigma_1^{cr} = K \left[\frac{1+r}{\sqrt{3(1+2r)}} \frac{t}{R_2} \sqrt{n} \alpha_1^{1-1/n} \right]^n$	$\varepsilon_1^{cr} = \frac{\sqrt{(1+2r)n}}{\sqrt{3}(1+r+\rho r)} \left(\frac{t}{R_2} \right)$
$\lambda_1^{cr^2} = \frac{2\sqrt{3}\sqrt{n}}{\frac{1+r}{\sqrt{1+2r}} - \frac{(1-n)\sqrt{1+2r}}{1+r}} \frac{1}{\alpha_1^2}$	$\lambda_1^{cr^2} = \frac{2\sqrt{3}\sqrt{n}}{\frac{1+r}{\sqrt{1+2r}} - \frac{(1-n)\sqrt{1+2r}}{1+r}} \frac{1}{\bar{\alpha}_1^2}$
<p>Swift's Law</p>	<p>Swift's Law</p>
$\sigma_1^{cr} = \frac{K}{2^n \alpha_1} \left[\varepsilon_o + \left[\varepsilon_o^2 + 4n\alpha_1^2 \frac{(1+r)^2}{3(1+2r)} \left(\frac{t}{R_2} \right)^2 \right]^{1/2} \right]^n$	$\varepsilon_1^{cr} = \frac{1}{2\bar{\rho}_1} \left[\left[\varepsilon_o^2 + 4n\bar{\alpha}_1^2 \frac{(1+r)^2}{3(1+2r)} \left(\frac{t}{R_2} \right)^2 \right]^{1/2} - \varepsilon_o \right]$
$\sigma_1^{cr} = \frac{K}{2^n \bar{\alpha}_1} \left[\varepsilon_o + \left[\varepsilon_o^2 + 4n\bar{\alpha}_1^2 \frac{(1+r)^2}{3(1+2r)} \left(\frac{t}{R_2} \right)^2 \right]^{1/2} \right]^n$	$\bar{\rho}_1 = \frac{1+r}{\sqrt{1+2r}} \left[1 + \frac{2\rho r}{1+r} + \rho^2 \right]^{1/2}$

$\varepsilon_p = \left(\frac{\alpha_1 \sigma_1^{cr}}{K} \right)^{1/n} - \varepsilon_o$ $E_t = K n (\varepsilon_p + \varepsilon_o)^{n-1}$ $E_s = \frac{K (\varepsilon_p + \varepsilon_o)^n}{\varepsilon_p}$ $\lambda_1^{cr^2} = \frac{2\sqrt{3} (1+r) \sqrt{E_s E_t}}{\sqrt{(1+2r)} \left[\frac{(1+r)^2}{1+2r} E_s - (E_s - E_t) \left(\frac{1}{\alpha_1} \right)^2 \right]}$ $L_1 = \frac{l}{\lambda_1} = \frac{\sqrt{R_2 t}}{\lambda_1}$ $f_\sigma = \frac{\sigma_1}{\sigma_1^{cr}}$ $L^w = \frac{L_1}{m} f_\sigma^{-1}$	$\varepsilon_p = \left(\frac{\bar{\alpha}_1 \sigma_1^{cr}}{K} \right)^{1/n} - \varepsilon_o$ $E_t = K n (\varepsilon_p + \varepsilon_o)^{n-1}$ $E_s = \frac{K (\varepsilon_p + \varepsilon_o)^n}{\varepsilon_p}$ $\lambda_1^{cr^2} = \frac{2\sqrt{3} (1+r) \sqrt{E_s E_t}}{\sqrt{(1+2r)} \left[\frac{(1+r)^2}{1+2r} E_s - (E_s - E_t) \left(\frac{1}{\bar{\alpha}_1} \right)^2 \right]}$ $L_1 = \frac{l}{\lambda_1} = \frac{\sqrt{R_2 t}}{\lambda_1}$ $f_\varepsilon = \frac{\varepsilon_1}{\varepsilon_1^{cr}}$ $L^w = \frac{L_1}{m} f_\varepsilon^{-1}$
--	--

Now, for wrinkling perpendicular to the 2-direction, we first note the relation between the proportionality factors in the 1 and 2 directions when used in the critical stress and strain evaluation

$$\sigma_e = \alpha_1 \sigma_1 = \alpha_2 \sigma_2 = \alpha_2 \alpha \sigma_1 \quad \Rightarrow \quad \alpha_2 = \frac{\alpha_1}{\alpha}$$

and in the same way

$$\sigma_e = \bar{\alpha}_1 \sigma_1 = \bar{\alpha}_2 \sigma_2 = \bar{\alpha}_2 \alpha \sigma_1 \quad \Rightarrow \quad \bar{\alpha}_2 = \frac{\bar{\alpha}_1}{\alpha}$$

finally

$$\varepsilon_e = \bar{\rho}_1 \varepsilon_1 = \bar{\rho}_2 \varepsilon_2 = \bar{\rho}_2 \rho \varepsilon_1 \quad \Rightarrow \quad \bar{\rho}_2 = \frac{\bar{\rho}_1}{\rho}$$

These relations can be used in case IV (Section 7) where the critical values have to be determined in both directions.

Stress	Strain
$\alpha = \sigma_1 / \sigma_2$	$\rho = \varepsilon_1 / \varepsilon_2$
$\alpha_2 = \left[1 - \frac{2r\alpha}{1+r} + \alpha^2 \right]^{1/2}$	$\bar{\alpha}_2 = \frac{\sqrt{1+2r}}{1+r+\rho r} \left[1 - \frac{2r\rho}{1+r} + \rho^2 \right]^{1/2}$
Hollomon's Law	Hollomon's Law
$\sigma_2^{cr} = K \left[\frac{1+r}{\sqrt{3(1+2r)}} \frac{t}{R_l} \sqrt{n} \alpha_2^{1-1/n} \right]^n$	$\varepsilon_2^{cr} = \frac{\sqrt{(1+2r)n}}{\sqrt{3} \left(1+r+\rho^{-1}r \right)} \left(\frac{t}{R_l} \right)$
$\lambda_2^{cr2} = \frac{2\sqrt{3} \sqrt{n}}{\frac{1+r}{\sqrt{1+2r}} - \frac{(1-n)\sqrt{1+2r}}{(1+r)} \frac{1}{\alpha_2^2}}$	$\lambda_2^{cr2} = \frac{2\sqrt{3} \sqrt{n}}{\frac{1+r}{\sqrt{1+2r}} - \frac{(1-n)\sqrt{1+2r}}{(1+r)} \frac{1}{\bar{\alpha}_2^2}}$
Swift's Law	Swift's Law
$\sigma_2^{cr} = \frac{K}{2^n \alpha_2} \left[\varepsilon_o + \left[\varepsilon_o^2 + 4n \alpha_2^2 \frac{(1+r)^2}{3(1+2r)} \left(\frac{t}{R_l} \right)^2 \right]^{1/2} \right]^n$	$\bar{\rho}_2 = \frac{(1+r)}{\sqrt{1+2r}} \left[1 + \frac{2\rho r}{1+r} + \rho^2 \right]^{1/2}$ $\varepsilon_2^{cr} = \frac{1}{2\bar{\rho}_2} \left[\left[\varepsilon_o^2 + 4n \bar{\alpha}_2^2 \frac{(1+r)^2}{3(1+2r)} \left(\frac{t}{R_l} \right)^2 \right]^{1/2} - \varepsilon_o \right]$
$\sigma_2^{cr} = \frac{K}{2^n \bar{\alpha}_2} \left[\varepsilon_o + \left[\varepsilon_o^2 + 4n \bar{\alpha}_2^2 \frac{(1+r)^2}{3(1+2r)} \left(\frac{t}{R_l} \right)^2 \right]^{1/2} \right]^n$	$\varepsilon_p = \left(\frac{\bar{\alpha}_2 \sigma_2^{cr}}{K} \right)^{1/n} - \varepsilon_o$
$\varepsilon_p = \left(\frac{\alpha_2 \sigma_2^{cr}}{K} \right)^{1/n} - \varepsilon_o$	$E_t = K n (\varepsilon_p + \varepsilon_o)^{n-1}$
$E_t = K n (\varepsilon_p + \varepsilon_o)^{n-1}$ $E_s = \frac{K (\varepsilon_p + \varepsilon_o)^n}{\varepsilon_p}$	$E_s = \frac{K (\varepsilon_p + \varepsilon_o)^n}{\varepsilon_p}$

$$\lambda_2^{cr,2} = \frac{2\sqrt{3}(1+r)\sqrt{E_s E_t}}{\sqrt{(1+2r)} \left[\frac{(1+r)^2}{1+2r} E_s - (E_s - E_t) \left(\frac{l}{\alpha_2} \right)^2 \right]}$$

$$L_2 = \frac{l}{\lambda_2} = \frac{\sqrt{R_1 t}}{\lambda_2}$$

$$f_\sigma = \frac{\sigma_2}{\sigma_2^{cr}}$$

$$L^w = \frac{L_2}{m} f_\sigma^{-1}$$

$$\lambda_2^{cr,2} = \frac{2\sqrt{3}(1+r)\sqrt{E_s E_t}}{\sqrt{(1+2r)} \left[\frac{(1+r)^2}{1+2r} E_s - (E_s - E_t) \left(\frac{l}{\bar{\alpha}_2} \right)^2 \right]}$$

$$L_2 = \frac{l}{\lambda_2} = \frac{\sqrt{R_1 t}}{\lambda_2}$$

$$f_\varepsilon = \frac{\varepsilon_2}{\varepsilon_2^{cr}}$$

$$L^w = \frac{L_2}{m} f_\varepsilon^{-1}$$

Appendix 2

The critical stresses and wave numbers, when the pre-wrinkling stress is used to determine the tangent and secant moduli for **Hollomon's law**, are given in both direction, by

$$\sigma_1^{cr} = K^{1/n} \left[\frac{1+r}{\sqrt{3(1+2r)}} \frac{t}{R_2} \sqrt{n} \alpha_1^{1-1/n} \right] \sigma_1^{1-1/n} \quad (\text{A2-1})$$

$$\sigma_2^{cr} = K^{1/n} \left[\frac{1+r}{\sqrt{3(1+2r)}} \frac{t}{R_1} \sqrt{n} \alpha_2^{1-1/n} \right] \sigma_2^{1-1/n} \quad (\text{A2-2})$$

$$\lambda_1^{cr,2} = \frac{2\sqrt{3} \sqrt{n}}{\frac{1+r}{\sqrt{1+2r}} - \frac{(1-n)\sqrt{1+2r}}{(1+r)} \frac{1}{\alpha_1^2}} \quad (\text{A2-3})$$

$$\lambda_2^{cr,2} = \frac{2\sqrt{3} \sqrt{n}}{\frac{1+r}{\sqrt{1+2r}} - \frac{(1-n)\sqrt{1+2r}}{(1+r)} \frac{1}{\alpha_2^2}} \quad (\text{A2-4})$$

To obtain the critical strains, we make use of the following relations

$$\sigma_e = K \varepsilon_e^n \quad \Rightarrow \quad \bar{\alpha}_1 \sigma_1^{cr} = K (\bar{\rho}_1 \varepsilon_1^{cr})^n \quad \text{and} \quad \bar{\alpha}_2 \sigma_2^{cr} = K (\bar{\rho}_2 \varepsilon_2^{cr})^n \quad (\text{A2-5})$$

to express the critical strains as

$$\varepsilon_1^{cr} = \frac{1}{\bar{\rho}_1} \left(\frac{\bar{\alpha}_1}{K} \right)^{1/n} \sigma_1^{cr,1/n} \quad (\text{A2-6})$$

$$\varepsilon_2^{cr} = \frac{1}{\bar{\rho}_2} \left(\frac{\bar{\alpha}_2}{K} \right)^{1/n} \sigma_2^{cr,1/n} \quad (\text{A2-7})$$

To evaluate the critical strains in terms of the principal strains, we first insert the following expressions of the principal stresses in (A2-1) and (A2-2)

$$\sigma_e = \bar{\alpha}_1 \sigma_1 = K (\bar{\rho}_1 \varepsilon_1)^n \quad \Rightarrow \quad \sigma_1 = K \frac{(\bar{\rho}_1 \varepsilon_1)^n}{\bar{\alpha}_1} \quad (\text{A2-8})$$

$$\sigma_e = \bar{\alpha}_2 \sigma_2 = K (\bar{\rho}_2 \varepsilon_2)^n \quad \Rightarrow \quad \sigma_2 = K \frac{(\bar{\rho}_2 \varepsilon_2)^n}{\bar{\alpha}_2} \quad (\text{A2-9})$$

Then, the resulting expressions of the critical stresses are inserted in (A2-6) and (A2-7).

Similarly to (A2-3) and (A2-4), the wave numbers are given by

$$\lambda_1^{cr2} = \frac{2\sqrt{3}\sqrt{n}}{\frac{1+r}{\sqrt{1+2r}} - \frac{(1-n)\sqrt{1+2r}}{(1+r)} \frac{1}{\bar{\alpha}_1^2}} \quad (\text{A2-10})$$

$$\lambda_2^{cr2} = \frac{2\sqrt{3}\sqrt{n}}{\frac{1+r}{\sqrt{1+2r}} - \frac{(1-n)\sqrt{1+2r}}{(1+r)} \frac{1}{\bar{\alpha}_2^2}} \quad (\text{A2-11})$$

when expressed in terms of strain proportionality factors.

Appendix 3

Curvatures Evaluation

Consider a point on a surface with normal vector (n) and tangent vectors (a_1, a_2) as shown in Figure A1. At this point we define the covariant metric tensor

$$[a] = \begin{bmatrix} a_1 \cdot a_1 & a_1 \cdot a_2 \\ a_2 \cdot a_1 & a_2 \cdot a_2 \end{bmatrix} \quad (\text{A3-1})$$

The curvature tensor is given by

$$[b] = - \begin{bmatrix} n_{,\xi} \cdot a_1 & n_{,\xi} \cdot a_2 \\ n_{,\eta} \cdot a_1 & n_{,\eta} \cdot a_2 \end{bmatrix} \quad (\text{A3-2})$$

The principal curvatures are the eigen values of the following eigen problem

$$[b] \begin{bmatrix} I \\ \lambda \end{bmatrix} - \frac{I}{R} [a] \begin{bmatrix} I \\ \lambda \end{bmatrix} = \begin{bmatrix} 0 \\ 0 \end{bmatrix} \quad (\text{A3-3})$$

where the matrix $[a]$ is symmetric and positive definite and $[b]$ is symmetric. Therefore, the eigen values $\frac{I}{R}$ and the eigen vectors $\begin{bmatrix} I \\ \lambda \end{bmatrix}$ are real values. It follows from (A3-3) that

the eigen values $\frac{I}{R_1}$ and $\frac{I}{R_2}$ are determined by

$$\det \left[[b] - \frac{I}{R} [a] \right] = 0 \quad (\text{A3-4})$$

or, simply

$$\left[\frac{I}{R} \right]^2 - 2H \left[\frac{I}{R} \right] + K = 0 \quad (\text{A3-5})$$

with the Gaussian curvature

$$K = \det \left[[b][a]^{-1} \right] = \det \left[\bar{b} \right] = \frac{1}{a} \det [b] \quad (\text{A3-6})$$

in which $a = \det [a]$

and the mean curvature

$$H = \frac{1}{2} \text{tr} \left[[b][a]^{-1} \right] = \frac{1}{2} \text{tr} \left[\bar{b} \right] \quad (\text{A3-7})$$

in which $\left[\bar{b} \right] = [b][a]^{-1}$.

Note that although $[a]$ and $[b]$ are symmetric $\left[\bar{b} \right]$ is not.

The roots of (A3-5) are the principal curvatures and are given by

$$\frac{1}{R_1} = H + \sqrt{H^2 - K} \quad \text{and} \quad \frac{1}{R_2} = H - \sqrt{H^2 - K} \quad (\text{A3-8})$$

which gives the following relations for the mean and Gaussian curvatures in terms of the principal curvatures

$$H = \frac{1}{2} \left(\frac{1}{R_1} + \frac{1}{R_2} \right) \quad \text{and} \quad K = \frac{1}{R_1 R_2} \quad (\text{A3-9})$$

In a finite element analysis context, the curvatures are evaluated from a finite element mesh consisting of low-order shell elements, as follows

- For each nodal point of the mesh all elements sharing this point are found.
- For each element the principal curvatures are evaluated in the following way

The normal unit vectors n are averaged from element normals (please refer to the shell depicted in Figure A2). The metric tensor is readily evaluated from the unit vectors a_1 and a_2 . The curvature tensor contains derivatives of the normal with respect to the shell coordinate directions which are approximated using the normals at nodes 2 and 3. Thus, the components of the curvature tensor are given by

$$\left. \begin{aligned} \bar{b}_{11} &= -\frac{\mathbf{n}_2 - \mathbf{n}_1}{l_{21}} \cdot \mathbf{a}_1 \\ \bar{b}_{22} &= -\frac{\mathbf{n}_3 - \mathbf{n}_1}{l_{31}} \cdot \mathbf{a}_2 \\ \bar{b}_{12} = \bar{b}_{21} &= -\frac{1}{2} \left[\frac{\mathbf{n}_3 - \mathbf{n}_1}{l_{31}} \cdot \mathbf{a}_1 + \frac{\mathbf{n}_2 - \mathbf{n}_1}{l_{21}} \cdot \mathbf{a}_2 \right] \end{aligned} \right\} \quad (\text{A3-10})$$

where l_{12} and l_{13} are the lengths of side 1-2 and 1-3, respectively.

Note that the last equation in (A3-10) is a symmetrisation of $\left[\bar{b} \right]$.

Finally (A3-6), (A3-7) and (A3-8) are used to determine the principal curvatures over each element.

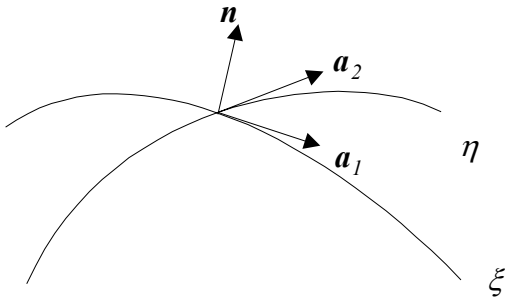


Figure A1. Unit normal and tangent vectors on a shell surface point.

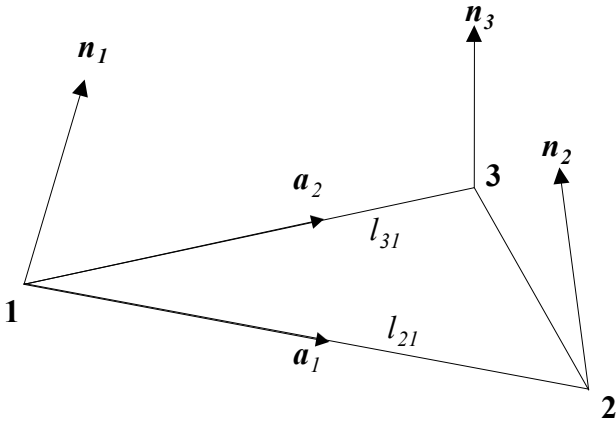


Figure A2. Triangular element with its locally defined normal and tangent vectors.

Appendix 4

The elements of the matrix M appearing in (8) are given by

$$M_{11} = \frac{l}{12} \left(\frac{t}{l} \right)^2 \left[L_{11} \lambda_1^4 + L_{22} \lambda_2^4 + 2(L_{12} + 2L_{44}) \lambda_1^2 \lambda_2^2 \right] + L_{11} \left(\frac{l}{R_1} \right)^2 + L_{22} \left(\frac{l}{R_2} \right)^2 + 2L_{12} \left(\frac{l}{R_1} \right) \left(\frac{l}{R_2} \right) - (\sigma_1 \lambda_1^2 + \sigma_2 \lambda_2^2) \quad (\text{A4-1})$$

$$M_{22} = L_{11} \lambda_1^2 + L_{44} \lambda_2^2 \quad (\text{A4-2})$$

$$M_{33} = L_{22} \lambda_2^2 + L_{44} \lambda_1^2 \quad (\text{A4-3})$$

$$M_{12} = M_{21} = L_{11} \lambda_1 \frac{l}{R_1} + L_{12} \lambda_1 \frac{l}{R_2} \quad (\text{A4-4})$$

$$M_{13} = M_{31} = L_{22} \lambda_2 \frac{l}{R_2} + L_{12} \lambda_2 \frac{l}{R_1} \quad (\text{A4-5})$$

$$M_{23} = M_{32} = (L_{12} + L_{44}) \lambda_1 \lambda_2 \quad (\text{A4-6})$$

where

$$L_{11} = \bar{L}_{1111} , L_{22} = \bar{L}_{2222} , L_{12} = \bar{L}_{1122} , L_{44} = \bar{L}_{1212} \quad (\text{A4-7})$$